

## A feasibility study to improve the processability of pure copper produced via laser powder bed fusion process

Abdollah Saboori<sup>1,\*</sup>, Marta Rocchetti Campagnoli<sup>2</sup>, Manuela Galati<sup>1</sup>,  
Flaviana Calignano<sup>1</sup>, Luca Iuliano<sup>1</sup>

<sup>1</sup> Integrated Additive Manufacturing Center, Department of Management and production Engineering, Politecnico di Torino, Corso duca Degli Abruzzi 24, 10129 Torino, Italy

<sup>2</sup> Department of Mechanical Engineering, Politecnico di Torino, Corso duca Degli Abruzzi 24, 10129 Torino, Italy

**Keywords:** Additive Manufacturing, Copper, Processability, Laser Powder Bed Fusion, Single Scan Tracks

**Abstract.** Additive Manufacturing (AM) refers to a family of layer-upon-layer building technologies capable of producing geometrically intricate parts in a single step. Today, the processability of many materials through AM is under development. One of the most interesting studies is the production of copper parts via laser-based technologies. Unluckily, mainly due to the high thermal conductivity and reflectivity of copper, its processability through AM processes is particularly challenging. Thus, in this research, a new material-based solution is proposed to improve the processability of copper through laser powder bed fusion. Therefore, a single scan track analysis is performed on pure copper and mixtures of copper/graphite. The outcomes show that adding graphite could increase copper's laser absorption and processability.

### Introduction

These days, thanks to the new developments in 3D printing technology, as well as the improvements achieved in equipment and materials, metal Additive Manufacturing (AM) has become one of the most attractive research fields [1,2]. However, this technology is classified into two main classes; Powder Bed Fusion (PBF) and Directed Energy Deposition (DED) [3–5]. It is well reported that, even if their manufacturing concept is the same, their building mechanisms are rather different. In the case of the PBF process, the laser melts the powder particles, which are already spread like a powder bed and solidify afterwards [6,7]. One of the key advantages of the AM processes is freedom in design that brings the complexity for free in the part design and production. Therefore, the production of complex shape parts, including the lattice structures or internal channels, was facilitated using metal AM processes [8,9]. A heat exchanger made of copper and copper alloys is one of these complex components that can be the first candidate to be produced via metal AM technologies [10].

Copper (Cu) which is a malleable and ductile metallic material, presents a good corrosion resistance and low chemical reactivity [11,12]. In addition, copper is characterised by extraordinary machinability, formability, and high electrical and thermal conductivity [13]. Copper attracts much attention in applications like microelectronics, roofs and plumbing implants, radiators, charge air coolers, and heat exchangers [14,15]. This wide range of characteristics and applications makes copper a promising material in various industrial sectors like electro packaging, automotive, and construction [16]. On the other hand, copper is also frequently used as a base material for different alloys such as brass and bronze, that, in addition to copper, consist of zinc and tin, respectively [17]. Owing to its high formability, copper is commonly processed via Powder Metallurgy (PM) or conventional manufacturing processes (e.g. forging, machining, extrusion and casting) [18]. However, these manufacturing techniques suffer from various limitations mainly related to the

difficulties in producing optimised finned heat exchangers and heat sinks [19]. As a matter of fact, traditional manufacturing processes for the complex components are characterised by high production costs as well as complex and time-consuming post-processing steps. The design of heat exchange components aims to minimise their size while using optimised thin fins to increase the surface area and the heat transfer rate between the heat exchanger surface and the surroundings [20]. In this context, AM processes results are attractive thanks to the possibility of producing topologically optimised geometries layer by layer, reducing the period of manufacturing and tooling requirements [2,18].

Despite the clear advantages of adopting AM technologies, it is well documented that the processability of copper and copper alloys via metal AM processes faces several challenges [18,21]. The high electrical and thermal conductivities of copper and its alloys increase the heat transfer rate from the melt pool to the surrounding area, generating high cooling rates and detrimental consequences for the process and the part quality [22]. In addition, for laser-based processes, the low laser absorption rate in the near-infrared region is another greatest issue. Both the rapid heat transfer and the high reflectivity that hinders the absorption of the laser power, result in high porosity and poor mechanical, thermal and electrical properties [18]. Moreover, the high sensitivity of copper to oxidation makes the powder handling of this alloy very difficult [21]. In fact, it requires an inert atmosphere during the process and special storage. The risk connected to the presence of copper oxides is the formation of gas bubbles inside the matrix of the final component, which reduces the density and electrical conductivity of the component.

Nevertheless, obtaining high-performance components following a layer-by-layer approach boosts wide scientific research to develop or enhance the processability of copper and its alloys through the AM processes [23]. Many works have been published in this context, particularly during the last years [24,25]. The adopted solutions can be grouped into technological-based or material based.

The technological-based solutions come back to modifying or optimising the design of machine or process parameters. For instance, Liu et al. succeeded to produced dense pure copper samples with a density of 99.6% using a blue laser [26]. Sciacca et al. also printed a dense pure copper heat sink through the LPBF process using the outcome of a process parameter optimization procedure [27]. Instead, material-based solutions concern the addition of other elements to the pure copper and/or the surface modification of the copper powder particles [18].

So far, several studies have been conducted to investigate the problems faced and present new possible solutions to be adopted. However, each alloy modification for the sake of processability increased the cost of the powder and also deteriorated some characteristics of the final components. Therefore, this paper aims to contribute to this growing area of research by proposing a new material-based solution to enhance the processability of copper to produce copper parts via laser-based AM technologies. Moreover, one of the main goals is to develop a new solution without increasing the cost and sacrificing some features, such as the thermal and electrical conductivity of copper components.

## **Materials and Methods**

A gas atomised spherical copper powder with a particle size range of 20-50  $\mu\text{m}$  and a graphite powder with an average particle size range of 7-11  $\mu\text{m}$  were used as the feedstock material.

In order to find the best graphite content from the flowability point of view, several powder mixtures containing different graphite contents were prepared in a low energy jar mill for 24 hours. Thereafter, the distribution of graphite powder within the copper particles was evaluated using a tabletop Scanning Electron Microscope (SEM, Phenom XL). The density, Hausner ratio (HR) and flowability of the powder mixtures were also assessed using a Hall flowmeter. The tapped density of powder mixtures was also evaluated using a container of 25  $\text{cm}^3$  that filled up till the highest compaction that was achieved through a vibration. Thereafter, the relative tapped density was

calculated using the theoretical density of the powder mixture. The same characterisations were also performed on the pure copper as a reference sample.

The spreadability of each composition was evaluated using a self-made spreading system that could simulate the powder spreading inside the LPBF machine. Then, the homogeneity of the powder layer was evaluated using a Leica Stereomicroscope.

Afterwards, two sets of single scan tracks (SSTs) with a length of 9 mm were produced for pure copper and Cu-0.5 wt.%C (Fig.1). For this reason, a design of experiment (DOE) consisting of 20 different combinations of process parameters was considered in this DOE, the laser power was between 85-95 W, and laser scanning speed was in the range of 100 to 250 mm/s, with a step size of 25 mm/s. The layer thickness was fixed at 0.02 mm. These combinations of process parameters resulted in a linear energy density in the range of 0.38 to 0.95 J/mm. The same DOE was used for pure copper to evaluate the role of graphite on the laser absorption of copper.

After the production, all the SSTs were analysed from the top using a Leica EZ4W stereomicroscope. Afterwards, two disks were cut, mounted and polished following the standard metallography reported for copper alloys. The as-polished surfaces were then etched chemically for further analysis by an optical microscope (OM). The geometry of the melt pools was measured from their cross-section using ImageJ software.

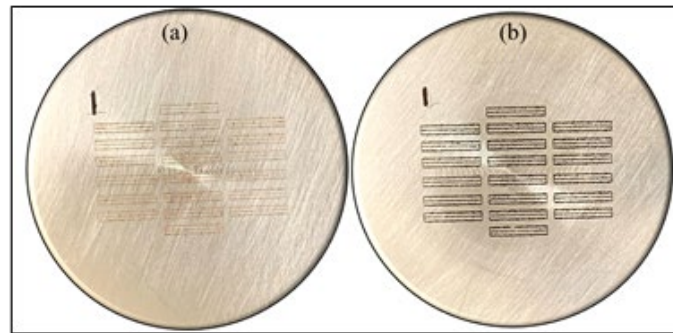


Fig. 1. (a) SSTs of pure coppers; (b) SSTs of Cu-0.5%C.

## Results and Discussions

### Powder characterisation

Fig. 2 shows the variation of relative tapped density of the Cu-C powder mixture as a function of graphite content. As can be seen, any addition of graphite to pure copper reduces the tapped density of the powder mixture and, consequently, the packing density of the powder layer.

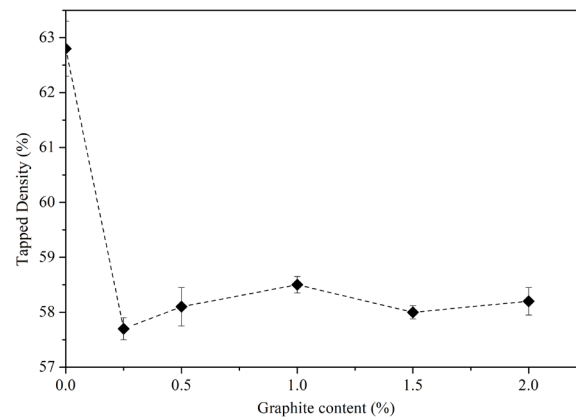


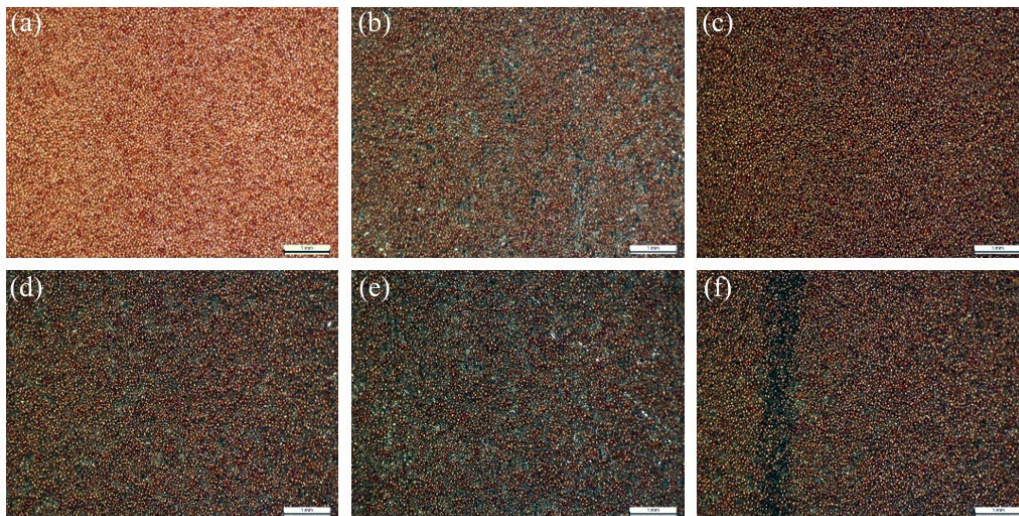
Fig. 2. Tapped density of Cu-C powder mixture as a function of graphite content.

Table 1 compares the Hausner ratio of the powder mixtures with pure copper. It is shown that pure copper with a proper Hausner ratio ( $1.0 < HR < 1.1$ ) exhibited excellent flowability. In contrast, the addition of graphite resulted in higher values ( $HR > 1.19$ ) and, as a consequence, poor flowability. The effect of graphite content on the flowability and spreadability of the copper powder is shown in Fig. 3, which compares a layer of copper powder with the powder mixtures.

*Table 1. The hausner ratio of pure copper and copper-graphite powder mixture.*

Composition (wt.%)	Hausner ratio
Pure Cu	1.10
Cu-0.25%C	1.14
Cu-0.5%C	1.20
Cu-1.0%C	1.22
Cu-1.5%C	1.25
Cu-2.0%C	1.26

This analysis confirmed the trends of the tapped density and Hausner ratio, decreasing the packing density and spreadability of the powder mixture as a function of the graphite content.



*Fig. 3. OM micrograph of a layer of (a) pure Cu, (b) Cu-0.25%C, (c) Cu-0.5%C, (d) Cu-1.0%C, (e) Cu-1.5%Cu, (f) Cu-2.0%C.*

As it is possible to see in Fig. 3, pure copper shows a perfect uniform distribution over the plate, thanks to the spherical shape of the particles. Adding a small quantity of graphite negatively affects the spreadability, and the mixture cannot fully cover the base plate. In the opposite case, if the amount of graphite surpasses 1.5 wt.%, it cannot mix homogeneously with the copper, forming agglomerates that deteriorate the uniformity of the powder layer. After that, the graphite distribution within the copper powder is evaluated through the SEM analysis, and the outcomes are reported in Fig. 4.

As can be seen in Fig. 4, the graphite plates adhered to the surface of copper particles, and they tended to form agglomerates as the graphite content increased and consequently deteriorated the flowability of the powder mixture.

Considering the outcomes of the powder characterisations, the composition of Cu-0.5%C was chosen as the most promising one for SSTs analysis. As mentioned earlier, the powder consisting of 0.5% graphite exhibited an acceptable tapped density and Hausner ratio than can guarantee the flowability of the powder mixture. Moreover, the spreadability test and SEM analysis confirmed that the spread powder layer is agglomerate free and uniform.



After printing the SSTs following the DOE considered in this research, it was possible to group the SSTs into four different categories: samples with not enough Linear Energy Density (LED), melt pools with evident balling, thin and stable or irregular SSTs (As shown in Fig. 5).

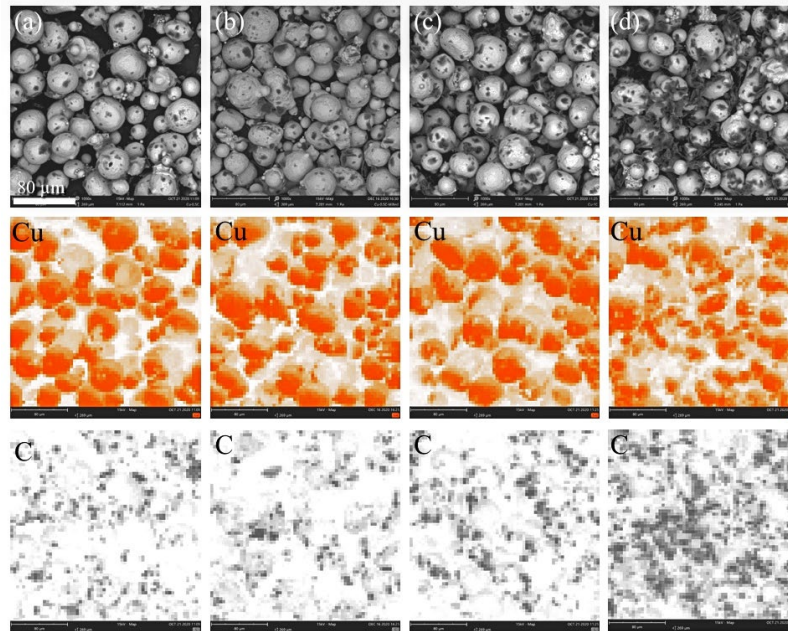


Fig. 4. SEM images of (a) Cu-0.5%C, (b) Cu-1.0%C, (c) Cu-1.5%C, (d) Cu-2.0%C.

No scan track was revealed in the “Not enough LED” case since the LED used was insufficient to melt the powder. In the second case, balling behaviour prevails: the scan track was discontinuous, and the melt pool is characterised by poor wetting. The “Thin and stable” category is individuated in a narrow range of LEDs, where the SSTs resulted in a uniform melt pool. Finally, the melt pools are strongly asymmetrical with higher LED values: these latter are defined as “Irregular”.

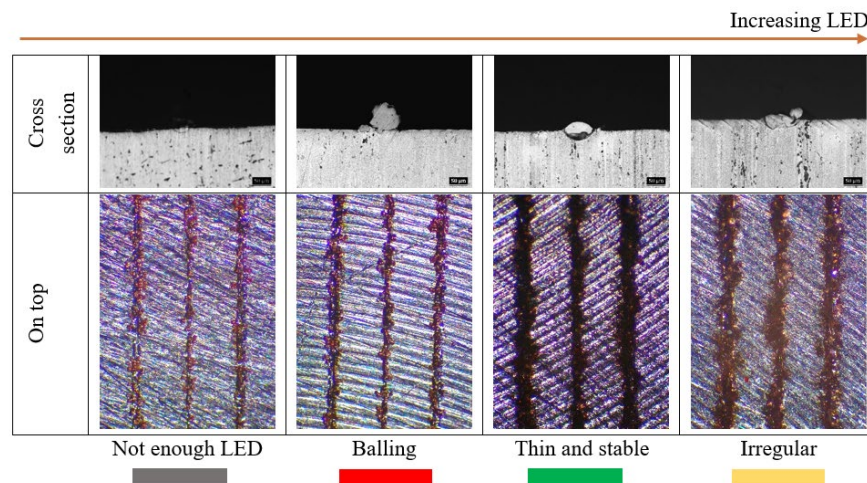


Fig. 5. Examples of different melt pools: not-enough LED, balling effect, thin and stable, irregular.

Fig. 6 demonstrates the cross-section of the SSTs of pure copper at different line energies. This figure shows that very high energy densities result in irregular melt pools, whereas very low line energies lead to unstable SSTs. However, as can be seen, thin and stable melt pools are formed at the medium level LED. On the other hand, it is clear that LED can not be considered a key factor

in finding the optimum process parameters. This means two sets of processes with the same line energy do not essentially form the same melt pool size. For instance, the LED of 0.422 J/mm resulted in an unstable melt pool, while the melt pool generated using other sets of parameters with the LED of 0.425 was regular and stable.

Fig. 7 shows the variation of the melt pool width of pure copper as a function of LED. This graph also confirms that the melt pool width can be different at the constant energy density. Interestingly, the melt pools are quite small with a LED ranging between 0.4 and 0.5 J/mm, and the scan tracks are just fairly continuous. The increment in LED starts to be detrimental when it exceeds the value of 0.7 J/mm.

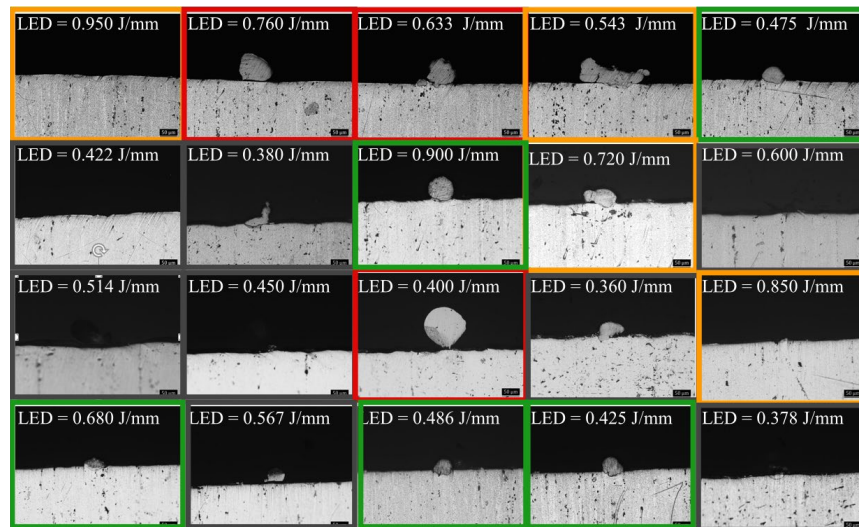


Fig. 6. Melt pool cross-section of pure copper SSTs.

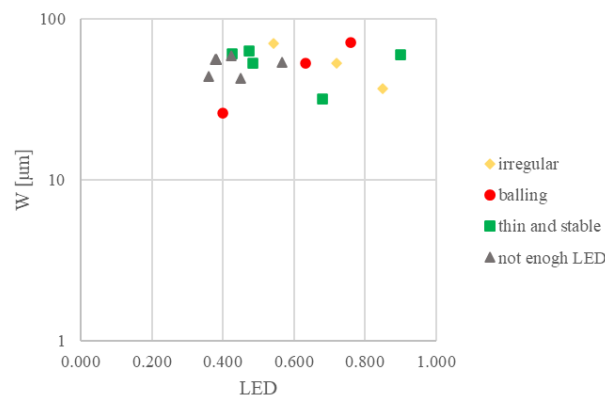


Fig. 7. Melt pool width of pure copper as a function of LED (J/mm).

Fig. 8 shows the cross-section of the Cu-0.5%C melt pools. As can be seen, after adding the graphite platelets, the undesired phenomena of balling reduced significantly, and the melt pools looked more stable.

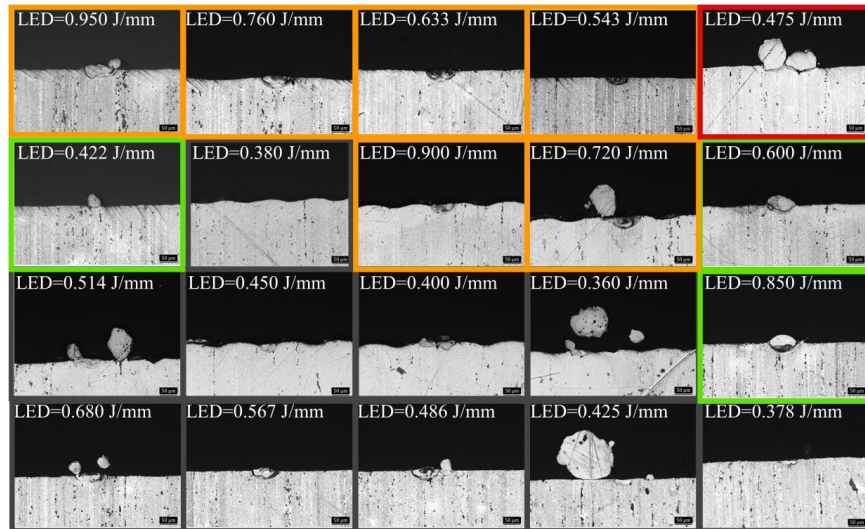


Fig. 8. Melt pool cross-section of Cu-0.5%C SSTs.

Fig. 9 compares the width of the Cu-0.5%C melt pool produced using different linear energy densities. This figure shows that as the melt pools result more stable with respect to the pure copper, the dimensions of the melt pools are larger, in particular the width of melt pools. This finding confirms that the addition of a small quantity of graphite could result in a higher LED absorption, consequently, the larger the melt pool formation.

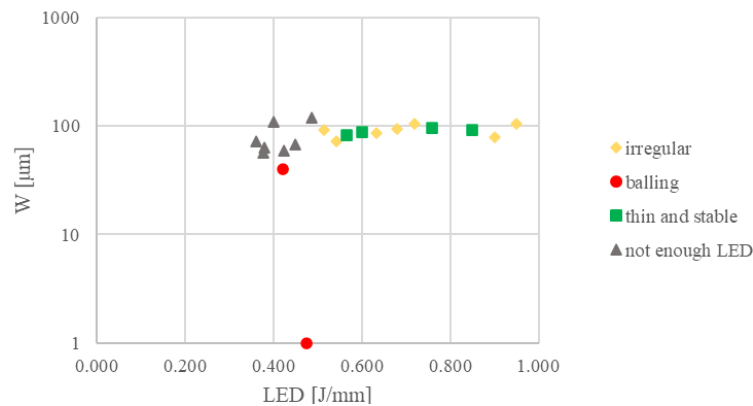


Fig. 9. Melt pool cross-section of Cu-0.5%C SSTs.

### Conclusions

In this study, the effects of adding different amounts of graphite to copper powder were analyzed. With its higher laser absorption, graphite helps improve copper manufacturing through laser based AM processes. In contrast, the quantity and the dimensions of graphite flakes need to be carefully selected so as not to destroy the mixture's spreadability. The outcomes demonstrated that the best quantity of graphite to be added is 0.5 wt.%. A good density, flowability, and spreadability can be obtained with this value. Moreover, high coverage of copper particles is ensured, and no graphite agglomerations are detected. A comparison between the cross-section of the SSTs of pure copper and Cu-0.5%C confirmed that the melt pools of the Cu-0.5%C generally look more stable and wider with respect to the pure copper ones. This suggests that the mixture can absorb a larger amount of LED, increasing the dimensions of the melt pools. This study lays the groundwork for future research into the successful fabrication of complex shape components through the LPBF process, thanks to the addition of a small quantity of graphite.

## References

- [1] M. Dadkhah, M.H. Mosallanejad, L. Iuliano, A. Saboori, A Comprehensive Overview on the Latest Progress in the Additive Manufacturing of Metal Matrix Composites: Potential, Challenges, and Feasible Solutions, *Acta Metall. Sin. (English Lett.* 34 (2021) 1173–1200. <https://doi.org/10.1007/s40195-021-01249-7>
- [2] M. Attaran, The rise of 3-D printing: The advantages of additive manufacturing over traditional manufacturing, *Bus. Horiz.* 60 (2017) 677–688. <https://doi.org/https://doi.org/10.1016/j.bushor.2017.05.011>
- [3] A. Saboori, A. Aversa, G. Marchese, S. Biamino, M. Lombardi, P. Fino, Application of Directed Energy Deposition-Based Additive Manufacturing in Repair, *Appl. Sci.* 9 (2019). <https://doi.org/10.3390/app9163316>
- [4] M.H. Mosallanejad, B. Niroumand, A. Aversa, D. Manfredi, A. Saboori, Laser Powder Bed Fusion in-situ alloying of Ti-5%Cu alloy: Process-structure relationships, *J. Alloys Compd.* 857 (2021) 157558. <https://doi.org/10.1016/j.jallcom.2020.157558>
- [5] I.O. for S. ISO/ASTM, ASTM 52900: 2015 (ASTM F2792) Additive Manufacturing—General Principles—Terminology, ISO Geneva, Switz. (n.d.).
- [6] M. Aristizabal, P. Jamshidi, A. Saboori, S.C. Cox, M.M. Attallah, Laser powder bed fusion of a Zr-alloy: Tensile properties and biocompatibility, *Mater. Lett.* 259 (2020) 126897. <https://doi.org/https://doi.org/10.1016/j.matlet.2019.126897>
- [7] M.H. Mosallanejad, B. Niroumand, A. Aversa, A. Saboori, In-situ alloying in laser-based additive manufacturing processes: A critical review, *J. Alloys Compd.* 872 (2021) 159567. <https://doi.org/https://doi.org/10.1016/j.jallcom.2021.159567>
- [8] G. Del Guercio, M. Galati, A. Saboori, Electron beam melting of Ti-6Al-4V lattice structures: correlation between post heat treatment and mechanical properties, *Int. J. Adv. Manuf. Technol.* 116 (2021) 3535–3547. <https://doi.org/10.1007/s00170-021-07619-w>
- [9] G. Del Guercio, M. Galati, A. Saboori, P. Fino, L. Iuliano, Microstructure and Mechanical Performance of Ti–6Al–4V Lattice Structures Manufactured via Electron Beam Melting (EBM): A Review, *Acta Metall. Sin. (English Lett.* 33 (2020) 183–203. <https://doi.org/10.1007/s40195-020-00998-1>
- [10] S.D. Jadhav, S. Dadbakhsh, J. Vleugels, J. Hofkens, P. Van Puyvelde, S. Yang, J.-P. Kruth, J. Van Humbeeck, K. Vanmeensel, Influence of Carbon Nanoparticle Addition (and Impurities) on Selective Laser Melting of Pure Copper, *Materials (Basel)*. 12 (2019) 2469. <https://doi.org/10.3390/ma12152469>
- [11] A. Saboori, M. Pavese, C. Badini, P. Fino, Development of Al- and Cu-based nanocomposites reinforced by graphene nanoplatelets: Fabrication and characterization, *Front. Mater. Sci.* 11 (2017). <https://doi.org/10.1007/s11706-017-0377-9>
- [12] A. Saboori, M. Pavese, C. Badini, P. Fino, A Novel Cu–GNPs Nanocomposite with Improved Thermal and Mechanical Properties, *Acta Metall. Sin. (English Lett.* 31 (2018) 148–152. <https://doi.org/10.1007/s40195-017-0643-y>
- [13] L. Kaden, G. Matthäus, T. Ullsperger, H. Engelhardt, M. Rettenmayr, A. Tünnermann, S. Nolte, Selective laser melting of copper using ultrashort laser pulses, *Appl. Phys. A.* 123 (2017) 596. <https://doi.org/10.1007/s00339-017-1189-6>



- [14] A. Saboori, S.K. Moheimani, M. Pavese, C. Badini, P. Fino, New Nanocomposite Materials with Improved Mechanical Strength and Tailored Coefficient of Thermal Expansion for Electro-Packaging Applications, *Met. (Basel)*. 7 (2017)
- [15] V. Sufiiarov, E. Borisov, I. Polozov, SELECTIVE LASER MELTING OF COPPER ALLOY, *Mater. Phys. Mech.* 43 (2020) 65–71. [https://doi.org/10.18720/MPM.4312020\\_8](https://doi.org/10.18720/MPM.4312020_8)
- [16] M.A. Lodes, R. Guschlbauer, C. Körner, Process development for the manufacturing of 99.94% pure copper via selective electron beam melting, *Mater. Lett.* 143 (2015) 298–301. <https://doi.org/https://doi.org/10.1016/j.matlet.2014.12.105>
- [17] A. Popovich, V. Sufiiarov, I. Polozov, E. Borisov, D. Masaylo, A. Orlov, Microstructure and mechanical properties of additive manufactured copper alloy, *Mater. Lett.* 179 (2016) 38–41. <https://doi.org/https://doi.org/10.1016/j.matlet.2016.05.064>
- [18] M. Rocchetti Campagnoli, M. Galati, A. Saboori, On the processability of copper components via powder-based additive manufacturing processes: Potentials, challenges and feasible solutions, *J. Manuf. Process.* 72 (2021) 320–337. <https://doi.org/https://doi.org/10.1016/j.jmapro.2021.10.038>
- [19] R. Neugebauer, B. Mueller, M. Gebauer, T. Töppel, Additive manufacturing boosts efficiency of heat transfer components, *Assem. Autom.* 31 (2011) 344–347. <https://doi.org/10.1108/01445151111172925>
- [20] L. Benedetti, C. Comelli, C. Ahrens, Study on Selective Laser Melting of Copper, 2017. <https://doi.org/10.26678/ABCM.COBEP2017.COF2017-0148>
- [21] T.I. El-Wardany, Y. She, V.N. Jagdale, J.K. Garofano, J.J. Liou, W.R. Schmidt, Challenges in Three-Dimensional Printing of High-Conductivity Copper, *J. Electron. Packag.* 140 (2018). <https://doi.org/10.1115/1.4039974>
- [22] F. Singer, D.C. Deisenroth, D.M. Hymas, M.M. Ohadi, Additively manufactured copper components and composite structures for thermal management applications, in: 2017 16th IEEE Intersoc. Conf. Therm. Thermomechanical Phenom. Electron. Syst., 2017: pp. 174–183. <https://doi.org/10.1109/ITHERM.2017.7992469>
- [23] T.Q. Tran, A. Chinnappan, J.K.Y. Lee, N.H. Loc, L.T. Tran, G. Wang, V. V Kumar, W.A.D.M. Jayathilaka, D. Ji, M. Doddamani, S. Ramakrishna, 3D printing of highly pure copper, *Metals (Basel)*. 9 (2019). <https://doi.org/10.3390/met9070756>
- [24] K. IMAI, T.-T. Ikeshoji, Y. SUGITANI, H. KYOGOKU, Densification of pure copper by selective laser melting process, *Mech. Eng. J.* (2020). <https://doi.org/10.1299/mej.19-00272>
- [25] F. Sciammarella, M. Gonser, M. Styrcula, Laser Additive Manufacturing of Pure Copper, 2013.
- [26] X. Liu, H. Wang, K. Kaufmann, K. Vecchio, Directed energy deposition of pure copper using blue laser, *J. Manuf. Process.* 85 (2023) 314–322. <https://doi.org/https://doi.org/10.1016/j.jmapro.2022.11.064>
- [27] G. Sciacca, M. Sinico, G. Cogo, D. Bigolaro, A. Pepato, J. Esposito, Experimental and numerical characterization of pure copper heat sinks produced by laser powder bed fusion, *Mater. Des.* 214 (2022) 110415. <https://doi.org/https://doi.org/10.1016/j.matdes.2022.110415>